LIMNOLOGY and OCEANOGRAPHY

ASLO

Limnol. Oceanogr. 70, 2025, 178–188

doi: 10.1002/lno.12752

Shifting phenology as a key driver of shelf zooplankton population variability

Isabel A. Honda,[1,2*] **Rubao Ji**,[1] **Gregory L. Britten**,[1,3] **Cameron Thompson**,[1,4] **Andrew R. Solow**,[1] **Zhengchen Zang**,[1,5,6,7] **Jeffrey A. Runge**[8]

[1]Biology Department, Woods Hole Oceanographic Institution, Woods Hole, Massachusetts, USA
[2]Department of Civil and Environmental Engineering, Massachusetts Institute of Technology, Cambridge, Massachusetts, USA
[3]Department of Earth, Atmospheric, and Planetary Sciences, Massachusetts Institute of Technology, Cambridge, Massachusetts, USA
[4]Northeastern Regional Association of Coastal Ocean Observing Systems, Portsmouth, New Hampshire, USA
[5]Department of Oceanography and Coastal Sciences, Louisiana State University, Baton Rouge, Louisiana, USA
[6]Center for Computation and Technology, Louisiana State University, Baton Rouge, Louisiana, USA
[7]Coastal Studies Institute, Louisiana State University, Baton Rouge, Louisiana, USA
[8]Darling Marine Center School of Marine Sciences, University of Maine, Walpole, Maine, USA

Abstract

The timing of biological events, known as phenology, plays a key role in shaping ecosystem dynamics, and climate change can significantly alter these timings. The Gulf of Maine on the Northeast U.S. Shelf is vulnerable to warming temperatures and other climate impacts, which could affect the distribution and production of plankton species sensitive to phenological shifts. In this study, we apply a novel data-driven modeling approach to long-term datasets to understand the population variability of *Calanus finmarchicus*, a lipid-rich copepod that is fundamental to the Gulf of Maine food web. Our results reveal how phenology impacts the complex intermingling of top-down and bottom-up controls. We find that early initiation of the annual phytoplankton bloom prompts an early start to the reproductive season for populations of *C. finmarchicus* in the inner Gulf of Maine, resulting in high spring abundance. This spring condition appears to be conducive to enhanced predation pressure later in the season, consequently resulting in overall low *C. finmarchicus* abundance in the fall. These biologically controlled dynamics are less pronounced in the outer Gulf of Maine, where water exchanges near the boundary have a greater influence. Our analysis augments existing hypotheses in fisheries oceanography and classical ecological theory by considering unique plankton life-history characteristics and shelf sea dynamics, offering new insights into the biological factors driving *C. finmarchicus* variability.

Phenology, or the study of cyclic variability and seasonal timings of biological events, plays a key role in shaping the dynamics of marine ecosystems. From the onset of blooms to the timing of migrations and occurrence of seasonal reproductive windows, understanding the phenology of a system offers invaluable insights into the potential biotic and abiotic factors driving population dynamics (Sydeman and Bograd 2009). Changing phenologies have long been identified in both terrestrial and marine systems and analyzed within the broader context of food web dynamics to develop ecological theories, understand the synchrony between predators and prey, and explain mortality patterns (Durant et al. 2007). Elucidating the drivers of shifting phenologies is becoming increasingly important as climate change continues to exert profound impacts on marine environments (Ji et al. 2010; Langan et al. 2021). Understanding these changes is crucial for advancing our knowledge of ecosystem structure, sensitivity, and resilience in a changing ocean.

The Gulf of Maine (Fig. 1), located on the Northwest Atlantic shelf, is warming at a rate faster than most global marine ecosystems and is projected to continue warming in the

*Correspondence: ihonda@mit.edu

Additional Supporting Information may be found in the online version of this article.

Author Contribution Statement: IAH and RJ conceptualized the idea for this study. IAH implemented the statistical analyses in consultation with GLB and ARS. ZZ formatted the chlorophyll *a* data. IAH and RJ interpreted results through discussion with CT and JAR. IAH wrote the original draft of the manuscript. All authors contributed to reviewing and revising the manuscript.

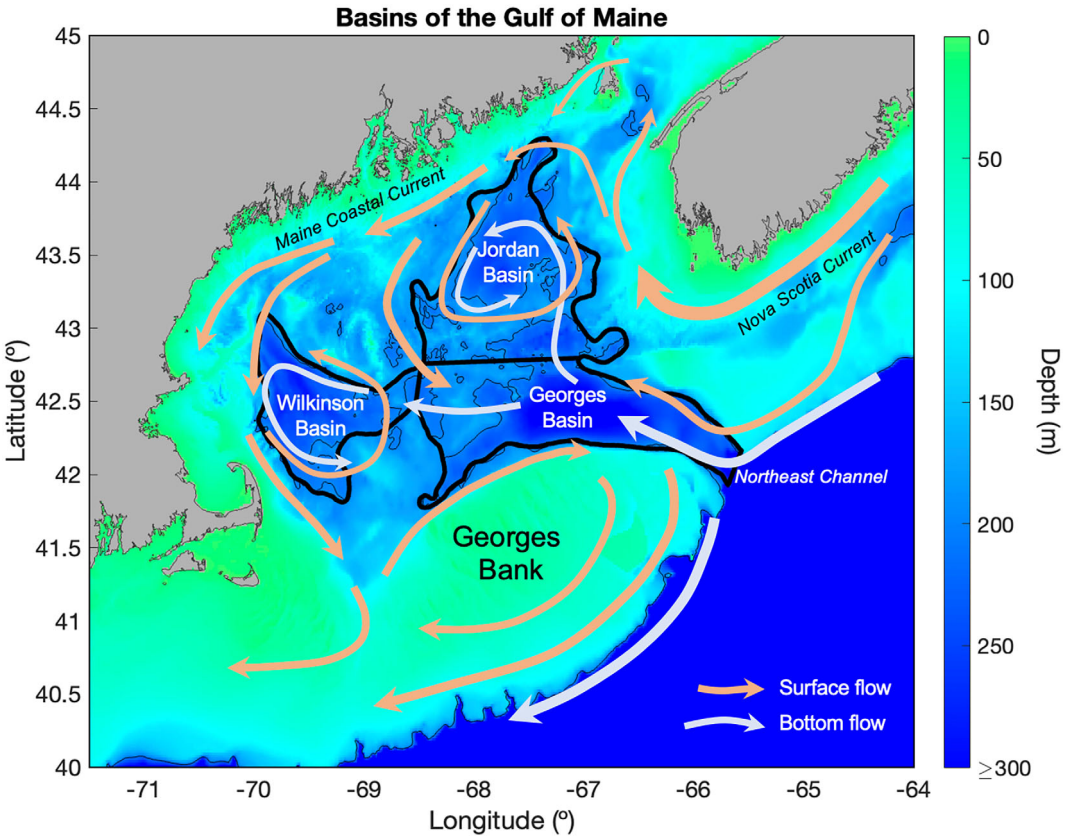

Fig. 1. Bathymetry of the Gulf of Maine with black boundaries representing the spatial areas of Wilkinson Basin, Jordan Basin, and Georges Basin. Directionality of average surface and bottom currents are indicated by orange and white arrows (respectively). Wilkinson Basin and Jordan Basin constitute the inner basins of the Gulf of Maine.

coming decades (see review by Pershing et al. 2021 and papers therein). This rapid and continued warming, along with shifting patterns of ocean circulation, is predicted to alter phenologies and the distribution of species in the region (Runge et al. 2015; Record et al. 2019). Of particular concern are the impacts these climate-induced changes will have on populations of the lipid-rich copepod, *Calanus finmarchicus*, which serves as a vital link between lower and higher trophic levels (Runge et al. 2015; Pershing et al. 2021). It is the primary prey species for the critically endangered North Atlantic right whale as well as many commercially and ecologically important fish species (Melle et al. 2014; Staudinger et al. 2020; Ross et al. 2023). Therefore, variability in *C. finmarchicus* populations, including phenological shifts and/or abundance changes, could have substantial impacts on the entire Gulf of Maine ecosystem.

To avoid visual predation and survive periods in which food is scarce, a key life-history strategy of *C. finmarchicus* is to diapause at depth in the basins of the Gulf of Maine (Meise and O'Reilly 1996). However, the timing and duration of diapause varies significantly from year to year, with predation cues, food availability, and increasing temperatures all impacting *C. finmarchicus* diapause schedules (Johnson et al. 2008; Ji 2011; Maps et al. 2012). Due to its complex multistage life cycle, uncertainties over the mechanisms triggering diapause, and other bottom-up and top-down controls that influence its population dynamics, modeling *C. finmarchicus* and understanding the mechanisms driving its spatiotemporal distribution remains a considerable challenge (Ji et al. 2021; Ratnarajah et al. 2023).

Although temperature and advection are important for *C. finmarchicus* growth and transport, recent studies suggest that these physical factors may not play as significant a role in driving spring *C. finmarchicus* population dynamics in the Gulf of Maine as was previously hypothesized (Ji et al. 2021; Honda et al. 2023). Both bottom-up and top-down biological processes could drive population variability, particularly during the winter–spring growing season. However, the relative importance of such internal biological processes, such as local food availability, reproductive timing, and predation pressure remains uncertain (Ji et al. 2021; Pershing and Kemberling 2023). To examine these potential biological mechanisms influencing *C. finmarchicus* variability, this study aims to link the phenology of the annual phytoplankton bloom to seasonal fluctuations of *C. finmarchicus* interannual abundance. We focus on bloom initiation date because it not only influences the start of *C. finmarchicus*'s reproductive season

and subsequent spring zooplankton biomass variability (Plourde and Runge 1993; Friedland et al. 2015, 2023), but also directly impacts bloom amplitude, duration, and food availability (Friedland et al. 2018). We hypothesize that the onset timing of the annual phytoplankton bloom plays a key role in driving *C. finmarchicus* population dynamics in the basins of the Gulf of Maine throughout the year, and we test this hypothesis through a novel analysis of the phenology of spring and fall population abundances and average late winter/early spring population stage structure in order to further elucidate the environmental drivers of a foundational species in the Gulf of Maine.

Methods

Our methods for this analysis are focused on estimating the average long-term seasonal trends of populations of *C. finmarchicus* using an unevenly distributed spatiotemporal dataset. We correlate seasonal average population abundances within the basins of the Gulf of Maine in order to analyze the influence of changes in phenology on population dynamics. We then link the timing of key seasonal events to potential drivers of variability, which change spatially across the region.

Data

This study utilizes publicly available plankton abundance data from the Marine Monitoring Assessment and Prediction (MARMAP) survey (1977–1987) and the Ecosystem Monitoring (EcoMon) program (1988 to the present) collected by the U.S. National Oceanic and Atmospheric Administration Northeast Fisheries Science Center (NMFS/NEFSC 2021). Approximate bimonthly samples were collected using a 61-cm bongo net with a 333-μm mesh towed between the surface to a maximum depth of 200 m at fixed stations (for MARMAP) or using a stratified random sampling design (for EcoMon). For the basins of the Gulf of Maine, there are varying degrees of seasonal representativity across all years, with the average number of spring/fall samples per basin per year ranging from approximately four to seven (Supporting Information Fig. S1). Despite the irregular spatiotemporal distribution of the data, based on a previous study, we ascertained that data collected within each of the three basins of the Gulf of Maine are interannually synchronized, indicating that subpopulations within each of these basins are varying in phase (Honda et al. 2023). Therefore, to analyze interannual trends, we aggregated the samples within the geographic boundaries representing Wilkinson, Jordan, and Georges Basin, as shown in Fig. 1.

The satellite surface chlorophyll *a* concentration data (Ocean Color Index algorithm) are the 8-d composite of MODIS-Terra chlorophyll *a* products from 2001 to 2019. The level-3 data with a 4-km spatial resolution were extracted from 35°N to 45°N and −76°W to −64°W for further analysis (NASA Ocean Biology Processing Group 2020).

Statistical approach

Our statistical approach is based on using generalized additive models (GAMs) to generate complete time series for each dataset and taking weighted seasonal averages to understand how seasonal abundances change interannually within each basin. First developed by Hastie and Tibshirani (1986), GAMs are a useful alternative to traditional multiple linear regression to model complex, non-linear ecological relationships, as they are able to capture additive smooth relationships and interactions between the response variable and the predictor variables, allowing for both flexibility and interpretability (Hastie and Tibshirani 1986; Pedersen et al. 2019).

We fitted all samples (i) collected within each basin (j) to the following GAM:

$$Y_{ij} = \beta_{ij} + s_{1j}(\mathrm{DoY}_{ij}) + s_{2j}(\mathrm{Year}_{ij}) + ti_{1j}(\mathrm{DoY}_{ij}, \mathrm{Year}_{ij}) + \varepsilon_{ij} \quad (1)$$

where β_{ij} is the intercept and covariates DoY_{ij} and Year_{ij} represent the day-of-year and year (respectively) of sample i in basin j. Smooth functions s_{1j} and s_{2j} model the direct effect of day-of-year and year on Y_{ij}, while $ti_{1j}(\mathrm{DoY}_{ij}, \mathrm{Year}_{ij})$ is a tensor interaction smooth for the interaction between day-of-year and year. Additionally, ε_{ij} represents normal error with mean 0 and variance σ^2. For plankton data, we take $Y_{ij} = ln(R_{ij})$, where R_{ij} is the total density of *C. finmarchicus* captured with the bongo net (mostly stages C3–C6, in units of $[(\text{abundance m}^{-3}) + 1]$. For chlorophyll *a* data, we take $Y_{ij} = ln(C_{ij})$, where C_{ij} is the concentration of chlorophyll *a*, in units of mg m^{-3}. In both cases, we utilized an identity link function to fit abundance/chlorophyll *a* concentration. Model fits and validation details are summarized in Supporting Information Table S1. All GAM analyses were performed using the "mgcv" R package (Wood 2017).

In order to more clearly discern trends in the unevenly distributed data, with the fitted model of Eq. 1, we generate a weekly time series ($\widehat{Y}$) with associated standard errors (SE) starting from January 1st of the first year of each dataset (i.e., 1977 for MARMAP/EcoMon and 2001 for MODIS-Terra chlorophyll *a*) to December 31st of the last year of each dataset (i.e., 2021 for MARMAP/EcoMon and 2019 for MODIS-Terra chlorophyll *a*). This interpolation was necessary because *C. finmarchicus* abundances can fluctuate significantly within short time frames, particularly in the spring, so our method aims to account for differences in the timing of sampling across years to effectively capture rapid changes in abundance. To incorporate uncertainty in the GAM-interpolated values, for each year (y) and season (s), we computed the weighted seasonal average ($\overline{Y}_{ys}$) according to Eq. 2:

$$\overline{Y}_{ys} = \frac{\sum_{t=t_0}^{t_f} \left(w_t \times \widehat{Y}\right)}{\sum_{t=t_0}^{t_f} w_t} \quad (2)$$

where $w_t = \frac{1}{SE_t^2}$ and t_0 and t_f represent the first and last day of the season (respectively) within the year. For this study, we define winter as ranging from day 1 to 90 (January to March), spring from day 91 to 181 (April to June), summer from day 182 to 273 (July to September), and fall from day 274 to 365 (October to December). We then estimated the Spearman's rank correlation (ρ) and associated p-value between weighted average seasonal *C. finmarchicus* population fluctuations and hypothesized drivers. To verify that these averages were representative of the data, we correlated the seasonal GAM averages with the seasonal MARMAP/EcoMon data averages. For all basins, the average seasonal interdecadal signals are positively correlated ($\rho > 0.32$) and statistically significant, with a confidence level of at least 90% (p-value < 0.1; Supporting Information Fig. S2).

Copepodite stage index calculation

To understand the mean copepodite stage composition of the *C. finmarchicus* population, we calculated the copepodite stage index (CSI) according to Eq. 3,

$$\mathrm{CSI} = \frac{\sum_{s=1}^{6} s \times c_s}{\sum_{s=1}^{6} c_s} \quad (3)$$

where s is the copepodite stage number from 1 to 6 and c_s is the abundance of stage s (Skjoldal et al. 2021). Here, we calculate CSI based on the available stage-resolved MARMAP/EcoMon data; however, the 333-μm mesh net used to collect these samples is more likely to catch stages C3–C6. In the late winter and early spring, high CSI indicates that there are more later stages than earlier stages, which suggests that the next generation of *C. finmarchicus* has not yet started to develop after emerging from diapause as late-stage copepodites. Conversely, a low CSI indicates that there are more earlier stages than older stages, which indicates that the reproduction/recruitment season of the population started earlier.

To investigate the hypothesis that an overall younger population in the late winter/early spring leads to high overall spring abundances, we determined the average stage composition (Eq. 3) of the population and correlated these values to overall average spring abundance. We calculated the average CSI from the 75th day-of-year to the 105th day-of-year within each year to match both the approximate bloom start date (D_C, defined in Eq. 4) and the 30-d timescale of reproduction, egg hatching, and population growth that occurs in the late winter and early spring following the annual phytoplankton bloom (Campbell et al. 2001).

Bloom initiation calculation

For each spatial location and year of the MODIS-Terra chlorophyll *a* data, we generated a complete daily time series of chlorophyll *a* seasonality and calculated bloom initiation date (D_C) as the day on which the maximum rate of increase occurs prior to day 120 of each year, as shown in Eq. 4:

$$D_C = \mathrm{argmax}_{t \le 120}\left(\frac{dC}{dt}(t)\right) \quad (4)$$

where $\frac{dC}{dt}$ represents the rate of change of chlorophyll *a* (C) with time (t) within each year. To avoid detection of short-lived spikes, we also enforced a condition that the overall concentration must exceed a threshold of 0.75 mg m^{-3} for 16 d. This threshold was chosen based on chlorophyll *a* conditions conducive to *C. finmarchicus* egg production (Durbin et al. 2003; Runge et al. 2006). Calculation of the overall D_C trend is not sensitive to this enforced condition, as combinations of 0.5–0.75 mg m^{-3} for 8 or 16 d did not alter the interannual variability of D_C (Supporting Information Fig. S3). This approach for calculating D_C is similar to the "Rate of Change Method" described by Brody et al. (2013), but has been modified to suit conditions favorable for *C. finmarchicus* egg development and reproduction in the Gulf of Maine to allow for detection of the late winter/early spring bloom even if chlorophyll *a* concentrations are relatively low but high enough for egg production. Unlike threshold-based methods, this approach ensures the early detection of the phytoplankton bloom, which is crucial for starting the reproductive season of *C. finmarchicus* (Head et al. 2000; Runge et al. 2006). For each basin, we took the mean D_C across all spatial locations (based on the spatial resolution of the MODIS-Terra chlorophyll *a* data) to estimate the average bloom initiation date for each year. Spatial bloom initiation maps for all three basins are found in Supporting Information Figs. S4–S6.

To test the hypothesis that CSI could be influenced by the phenology of the annual phytoplankton bloom, we calculated the average bloom initiation date (Eq. 4, D_C) across all basins and correlated this value with average CSI.

Results

Spring and fall population dynamics

There is a strong, statistically significant ($p < 0.01$), negative correlation between the weighted seasonal averages (Eq. 2) of the spring and fall populations in both Wilkinson Basin ($\rho = -0.83$) and Jordan Basin ($\rho = -0.80$) (Fig. 2). In contrast, the Georges Basin rank correlation between spring and fall weighted seasonal averages has a positive correlation that is weaker, but still statistically significant ($\rho = 0.44$; $p < 0.01$). Refer to Supporting Information Fig. S7 for plots of the seasonal average correlations of the raw MARMAP/EcoMon data compared to GAM average correlations.

Spring population vs. CSI

Spring abundances and CSI display statistically significantly negative relationships in the inner basins (Fig. 3), with the dynamics in Wilkinson Basin having $\rho = -0.82$ and $p < 0.01$, and Jordan Basin having $\rho = -0.31$ and $p = 0.05$. In contrast, correlations in Georges Basin are negative but not significant at the 95% confidence level ($\rho = -0.21$; $p = 0.17$).

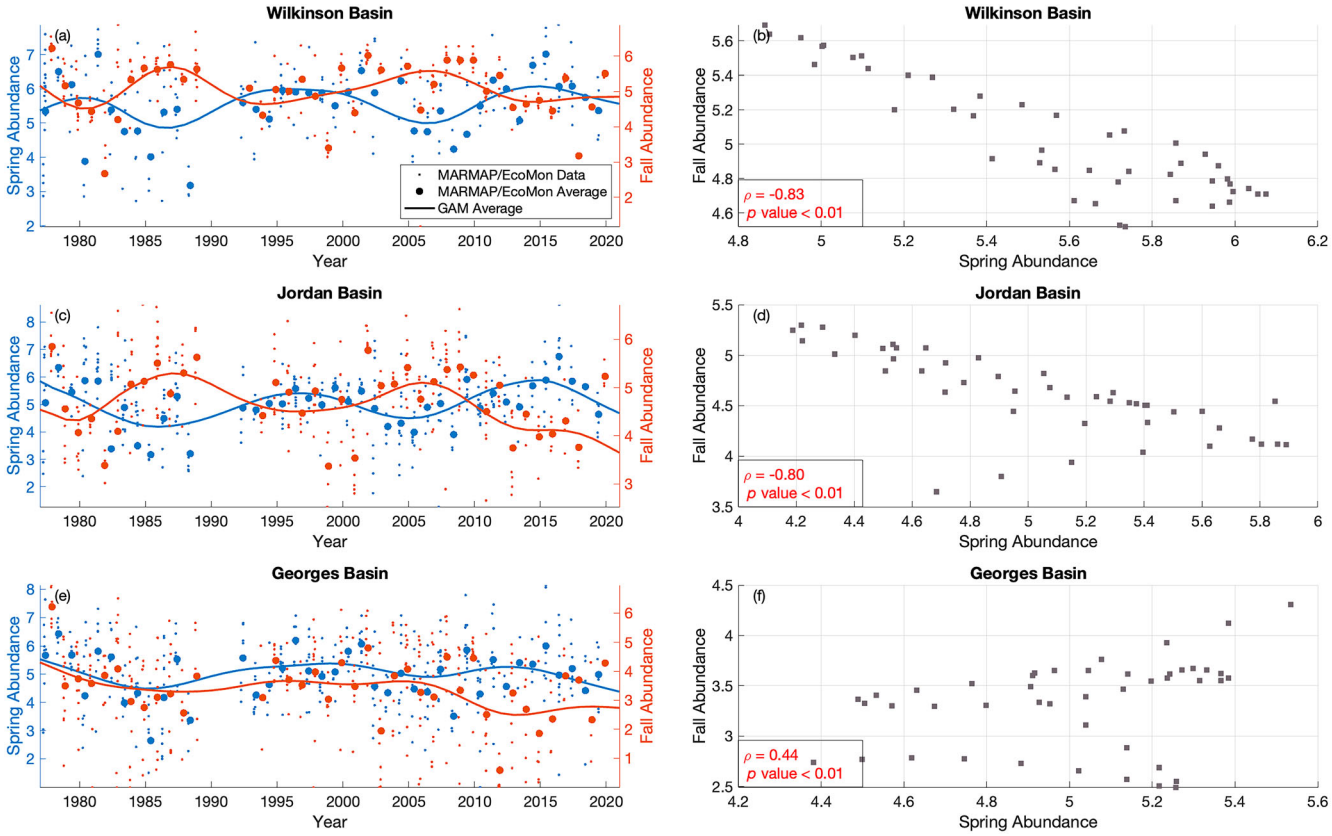

Fig. 2. Annual spring and fall data, averages, and trends within the basins of the Gulf of Maine. Left-hand panels show Marine Monitoring Assessment and Prediction (MARMAP)/Ecosystem Monitoring (EcoMon) samples collected within each basin (small circles) and MARMAP/EcoMon data seasonal averages (large circles), as well as generalized additive model (GAM)–derived seasonal averages (lines). Right-hand panels display scatter plots with Spearman's rank correlation ρ values and associated p-values for each basin. Abundances are in units of ln(abundance $m^{-3} + 1$).

CSI vs. spatial average bloom initiation

Bloom initiation date and CSI are significantly positively correlated (Fig. 4) in Wilkinson Basin ($\rho = 0.56$; $p = 0.01$) and Jordan Basin ($\rho = 0.77$; $p < 0.01$). This indicates that the timing of the annual phytoplankton bloom may play a key role in prompting an early start to the reproductive season in the inner Gulf of Maine, as early initiation corresponds with low CSI in a particular year. Conversely, Georges Basin does not display a significant relationship between these variables ($\rho = 0.14$; $p = 0.58$).

Discussion

Across the interconnected basins of the Gulf of Maine, a complex array of factors shape the population dynamics of *C. finmarchicus*, reflecting the intricate interplay between local biotic influences and broader advective processes. Despite the relatively close spatial proximity of the basins and high advective connectivity, our results show that the dynamics in each of the basins differs, but that Wilkinson Basin and Jordan Basin exhibit a higher degree of similarity with each other than with Georges Basin. This indicates that comparable seasonal biological mechanisms are driving the observed spatial population synchrony, as both basins are influenced by upstream shelf water at the surface, leading to similar winter–spring hydrographic conditions and biological production responses (Fig. 1) (Ji et al. 2017; Ji et al. 2021; Honda et al. 2023). In contrast, Georges Basin exhibits different dynamics, with populations in this basin showing much greater variability and displaying a positive correlation between spring and fall abundances and a weaker, negative correlation between spring abundance and CSI (Figs. 2f, 3c). This difference is likely attributed to the fact that the Georges Basin diapausing population is more directly influenced by exchanges at the boundary with external waters via the Northeast channel (Fig. 1). Although the entire Gulf of Maine is interconnected and can be influenced by these water masses, it takes a longer amount of time for this water to enter the inner basins of the Gulf of Maine, so Jordan and Wilkinson Basins are less influenced by these intrusions than Georges Basin (Ji et al. 2021). Thus, external processes likely play a more important role in driving population dynamics in Georges Basin, while similar biological drivers primarily influence the dynamics of Wilkinson and Jordan Basins.

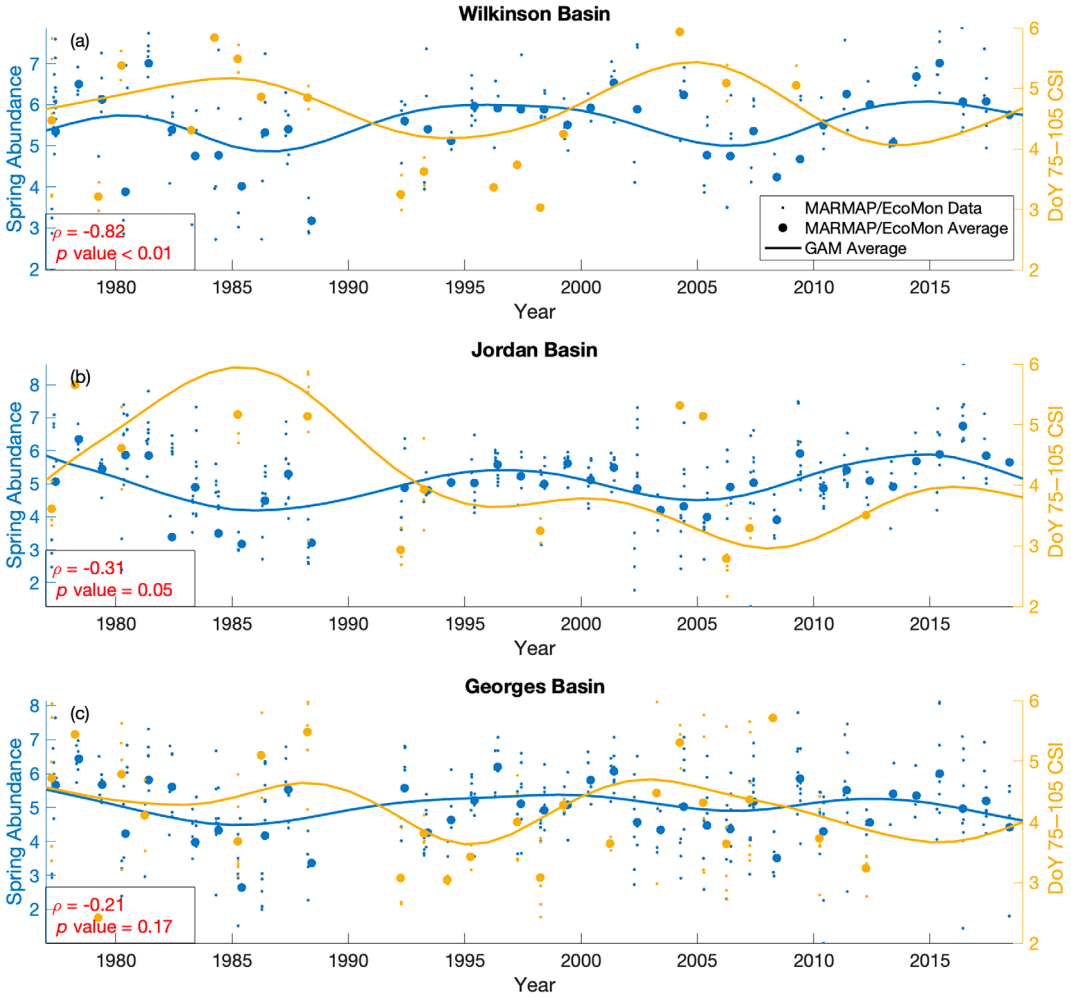

Fig. 3. Average spring abundance (units of ln[abundance $m^{-3} + 1$]) compared to average copepodite stage index (CSI) from the 75th day-of-year (DoY) to the 105th DoY for each year. Marine Monitoring Assessment and Prediction (MARMAP)/Ecosystem Monitoring (EcoMon) samples collected within each basin are indicated by small circles, MARMAP/EcoMon data seasonal averages are indicated by large circles, and generalized additive model (GAM)–derived seasonal averages are represented by lines. Spearman's rank correlation ρ values and associated p values are denoted in the lower left-hand corner of each plot.

For the inner basins of the Gulf of Maine, our results indicate that the phenology of annual biological events plays a key role in shaping population dynamics throughout the year. The positive correlation between bloom initiation date and CSI in Wilkinson and Jordan Basins (Fig. 4) supports our hypothesis that early bloom initiation prompts an early start to the reproductive season, as indicated by low average CSI. Furthermore, the negative correlation between CSI and spring abundance indicates that the earlier start to the reproductive cycle in late winter/early spring leads to high overall abundance in the spring. These dynamics could potentially be explained by the growth-mortality hypothesis, commonly explored in fisheries science (e.g., Anderson 1988; Davis et al. 1991), and more recently suggested to apply to *C. finmarchicus* (Ji et al. 2021). Our analyses show strong evidence that early bloom initiation prompts an early start to the reproductive season, allowing more time for the next generation of young copepodites to grow in size before smaller zooplanktonic predators have had time to peak. This results in a mismatch between *C. finmarchicus* peak abundance and peak abundance in predators later in the year and allows for overall high spring abundance, as illustrated in Fig. 5 (top panel) and Supporting Information Fig. S8.

Following a particularly high spring abundance season, our findings reveal a subsequent decline in fall abundance, as evidenced by the strong negative correlation observed between spring and fall abundances in Wilkinson Basin and Jordan Basin (Fig. 2b,d). This phenomenon could be interpreted in the context of the Lotka-Volterra model of density-dependent predator–prey interactions (Volterra 1926). According to this model, high surface populations of copepod prey (e.g., *C. finmarchicus*) provides ample food for predators, consequently fostering their reproduction and leading to an increase in predator abundance during the summer and fall

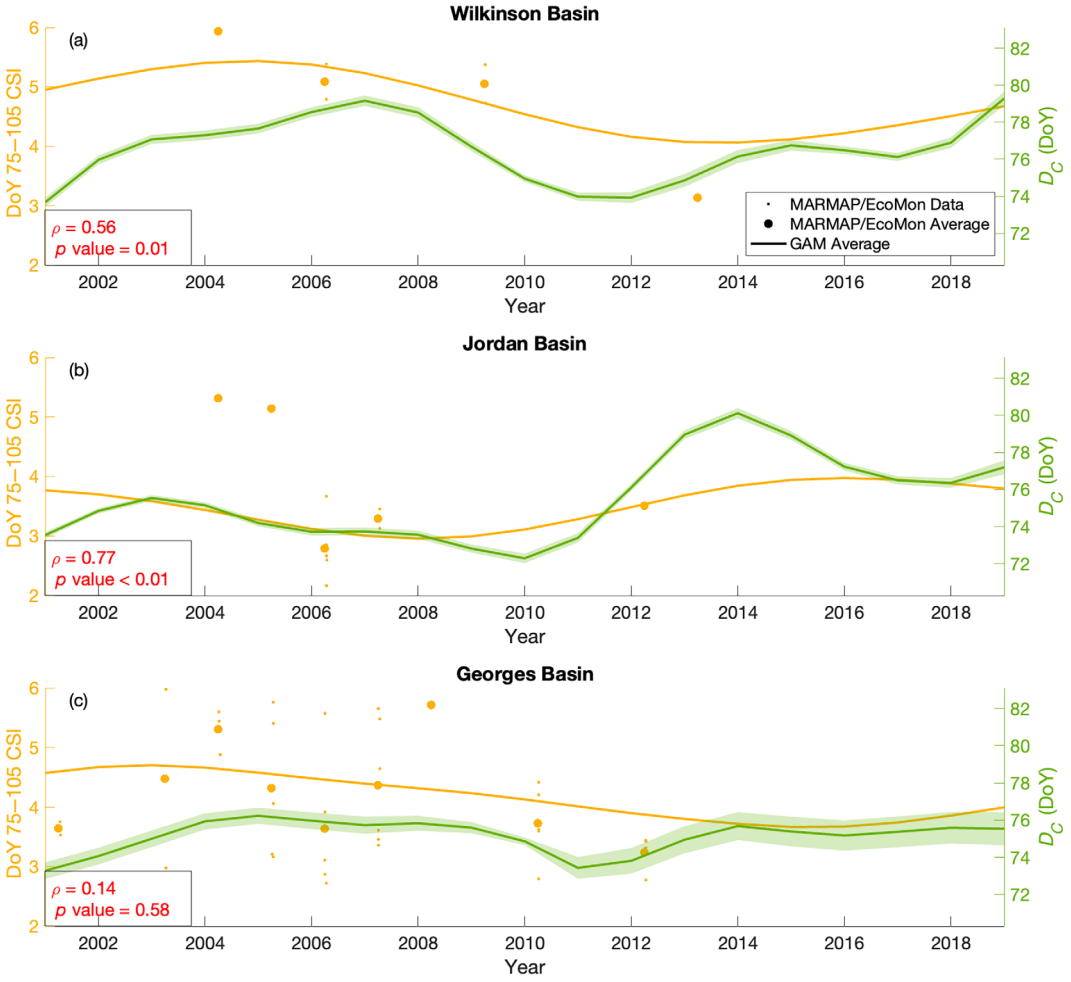

Fig. 4. Average copepodite stage index (CSI) from the 75th day-of-year (DoY) to the 105th DoY for each year compared to spatially averaged bloom initiation date (D_C). Marine Monitoring Assessment and Prediction (MARMAP)/Ecosystem Monitoring (EcoMon) samples collected within each basin are indicated by small circles, MARMAP/EcoMon data seasonal averages are indicated by large circles, and generalized additive model (GAM)–derived seasonal averages are represented by lines. The 95% confidence intervals for spatial average D_C are indicated by the shaded green envelope. Spearman's rank correlation ρ values and associated p values are denoted in the lower left-hand corner of each plot.

seasons. This increase in the predator population exerts heightened top-down pressure on *C. finmarchicus*, resulting in a subsequent decline in their abundance during the fall months. Simple Lotka-Volterra model results further support the presence of density-dependent predator–prey interactions in the inner Gulf of Maine (Supporting Information Fig. S8). However, since *C. finmarchicus* has a number of location-dependent and migrating predators ranging from invertebrates (e.g., euphausiids, chaetognaths, siphonophores), to fish (e.g., larval Atlantic cod, herring), to large mammals (e.g., the North Atlantic right whale), it is difficult to quantify total predation-induced mortality and identify specific predators most responsible for driving down *C. finmarchicus* populations (Ohman and Hirche 2001; Meyer-Gutbrod and Greene 2018; Wiebe et al. 2022). Thus, analyzing *C. finmarchicus* spring and fall abundances allows us to estimate overall *C. finmarchicus* mortality within the year, and our results suggest that that density-dependent predation could be an important factor driving *C. finmarchicus* population dynamics.

Another significant mechanism that could impact *C. finmarchicus* interannual population variability is the timing of diapause initiation in the summer and fall months, which could also result in low fall abundance. Early bloom initiation allows *C. finmarchicus* eggs to hatch earlier, and individuals in the population would then be able to develop and accumulate lipids sooner, which may prompt an early descent into diapause in the summer or early fall (Johnson et al. 2008; Maps et al. 2012). The complex interaction between food availability and predation pressure could also be an important factor in the initiation of diapause, as low summer food availability, as well as enhanced predation, could induce *C. finmarchicus* to enter diapause (Ji 2011; Skottene et al. 2020; Kvile et al. 2021). Once diapausing at depth, *C. finmarchicus* metabolizes the lipids acquired at the surface, and the rate of respiration

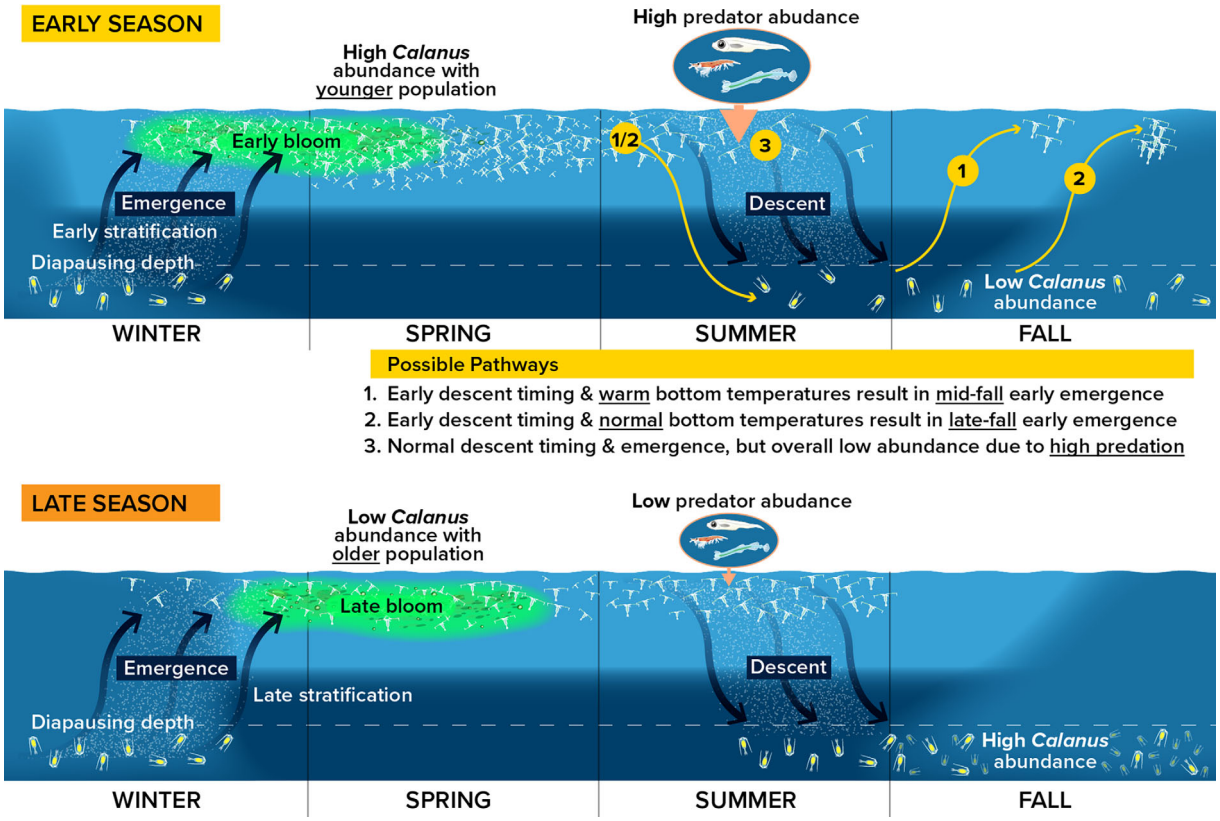

Fig. 5. Conceptual diagram depicting hypothesized conditions leading to observed spring and fall population dynamics within a particular year.

increases with water temperature (Fields et al. 2023). Low temperatures (i.e., below 5°C) allow for normal respiration rates and a full diapause duration. However, since lipid storage is limited and the population initially descended into diapause early, individuals may consequently emerge from diapause early (i.e., in the mid to late fall) (Maps et al. 2012). This would likely lead to increased mortality due to predation, advection out of the system due to greater surface currents, and a mismatch between emergence from diapause and food availability, all of which would result in reduced abundances in the fall (Sorochan et al. 2021). Additionally, higher sea bottom temperatures during the summer and fall could result in elevated metabolism (e.g., Saumweber and Durbin (2006); Pierson et al. (2013)), forcing an even earlier exit from the diapause phase and consequently leading to a higher mortality rate from higher temperatures, food scarcity, and increased predation pressure at the surface (Ji et al. 2021). These potential pathways leading to low fall abundance of *C. finmarchicus* are outlined in Fig. 5 (top panel). In short, complex interactions between both bottom-up and top-down pressures can consequently lead to fewer individuals in the fall following a high spring abundance season.

Understanding the phenology of a system can lend insights into the intricate interplay of top-down and bottom-up forcing on population dynamics. Through our analysis linking the phenology of bloom initiation to CSI fluctuations, our results suggest that the timing of the annual phytoplankton bloom and availability of food in the late winter/early spring may serve as crucial factors influencing *C. finmarchicus* abundance throughout the year, resulting in significant impacts to species interactions and overall ecosystem dynamics. Furthermore, the long term cyclic pattern between spring and fall abundance indicates a primary role for the interaction between spawning phenology and local predation in controlling the dynamics of *C. finmarchicus*, particularly for the inner basins of the Gulf of Maine, where fall population abundance could also be influenced by the summer advective supply from the Maine Coastal Current originating from the Scotian Shelf (Ji et al. 2017). Predicting the relative role of internal production vs. supply in the wake of climate change remains a challenge, and it is unclear how further freshening and warming may impact the system (Record et al. 2024). While recent bottom temperature increases have corresponded to a decrease in fall abundance in Jordan and Georges Basin, the signal was inconsistent in previous decades, and overall bottom temperature variability across the basins is irregular (Supporting Information Fig. S9). It remains to be seen whether the most recent oceanographic shift associated with the northward migration of

the Gulf Stream and change of supply of *C. finmarchicus* into the Gulf of Maine (Record et al. 2019; Meyer-Gutbrod et al. 2021) will radically alter the observed long term pattern. Since *C. finmarchicus* is a foundational species in the North Atlantic food web, understanding its seasonality and the environmental conditions driving changes in its abundance and distribution is essential for predicting the impacts of climate change on marine populations in the region.

Data availability statement

Plankton abundance data were collected by the MARMAP/EcoMon survey program, publicly available at the U.S. National Oceanic and Atmospheric Administration National Centers for Environmental Information site (https://www.ncei.noaa.gov/archive/accession/0187513; see NMFS/NEFSC 2021). MODIS-Terra chlorophyll *a* data is publicly available at the NASA MODIS site (https://modis.gsfc.nasa.gov/data/dataprod/chlor_a.php; see NASA Ocean Biology Processing Group 2020). R and MATLAB scripts used to conduct the statistical analyses are available at https://github.com/iahonda/Shifting-Phenology.git.

References

Anderson, J. T. 1988. A review of size dependent survival during pre-recruit stages of fishes in relation to recruitment. J. Northwest Atl. Fish. Sci. **8**: 55–66.

Brody, S. R., M. S. Lozier, and J. P. Dunne. 2013. A comparison of methods to determine phytoplankton bloom initiation. J. Geophys. Res. Oceans **118**: 2345–2357.

Campbell, R. G., M. M. Wagner, G. J. Teegarden, C. A. Boudreau, and E. G. Durbin. 2001. Growth and development rates of the copepod *Calanus finmarchicus* reared in the laboratory. Mar. Ecol. Prog. Ser. **221**: 161–183.

Davis, C. S., G. R. Flierl, P. H. Wiebe, and P. J. S. Franks. 1991. Micropatchiness, turbulence and recruitment in plankton. J. Mar. Res. **49**: 109–151.

Durant, J. M., D. O. Hjermann, G. Ottersen, and N. C. Stenseth. 2007. Climate and the match or mismatch between predator requirements and resource availability. Climate Res. **33**: 271–283.

Durbin, E., R. Campbell, M. Casas, M. Ohman, B. Niehoff, J. Runge, and M. Wagner. 2003. Interannual variation in phytoplankton blooms and zooplankton productivity and abundance in the Gulf of Maine during winter. Mar. Ecol. Prog. Ser. **254**: 81–100.

Fields, D. M., and others. 2023. A positive temperature-dependent effect of elevated CO_2 on growth and lipid accumulation in the planktonic copepod, *Calanus finmarchicus*. Limnol. Oceanogr. **68**: S87-S100.

Friedland, K. D., and others. 2015. Spring bloom dynamics and zooplankton biomass response on the US Northeast Continental Shelf. Cont. Shelf Res. **102**: 47–61.

Friedland, K. D., C. B. Mouw, R. G. Asch, A. S. A. Ferreira, S. Henson, K. J. W. Hyde, R. E. Morse, A. C. Thomas, and D. C. Brady. 2018. Phenology and time series trends of the dominant seasonal phytoplankton bloom across global scales. Glob. Ecol. Biogeogr. **27**: 551–569.

Friedland, K. D., N. R. Record, D. E. Pendleton, W. M. Balch, K. Stamieszkin, J. R. Moisan, and D. C. Brady. 2023. Asymmetry in the rate of warming and the phenology of seasonal blooms in the Northeast US Shelf Ecosystem. ICES J. Mar. Sci. **80**: 775–786.

Hastie, T., and R. Tibshirani. 1986. Generalized additive models. Stat. Sci. **1**: 297–310.

Head, E., L. Harris, and R. Campbell. 2000. Investigations on the ecology of *Calanus* spp. in the Labrador Sea. I. Relationship between the phytoplankton bloom and reproduction and development of *Calanus finmarchicus* in spring. Mar. Ecol. Prog. Ser. **193**: 53–73.

Honda, I. A., R. Ji, and A. R. Solow. 2023. Spatially varying plankton synchrony patterns at seasonal and interannual scales in a well-connected shelf sea. Limnol. Oceanogr. Letters **8**: 906–915.

Ji, R. 2011. *Calanus finmarchicus* diapause initiation: New view from traditional life history-based model. Mar. Ecol. Prog. Ser. **440**: 105–114.

Ji, R., M. Edwards, D. L. Mackas, J. A. Runge, and A. C. Thomas. 2010. Marine plankton phenology and life history in a changing climate: Current research and future directions. J. Plankton Res. **32**: 1355–1368.

Ji, R., Z. Feng, B. T. Jones, C. Thompson, C. Chen, N. R. Record, and J. A. Runge. 2017. Coastal amplification of supply and transport (CAST): A new hypothesis about the persistence of *Calanus finmarchicus* in the Gulf of Maine. ICES J. Mar. Sci. **74**: 1865–1874.

Ji, R., J. A. Runge, C. S. Davis, and P. H. Wiebe. 2021. Drivers of variability of *Calanus finmarchicus* in the Gulf of Maine: Roles of internal production and external exchange. ICES J. Mar. Sci. **0**: 1–10.

Johnson, C. L., A. W. Leising, J. A. Runge, E. J. H. Head, P. Pepin, S. Plourde, and E. G. Durbin. 2008. Characteristics of *Calanus finmarchicus* dormancy patterns in the Northwest Atlantic. ICES J. Mar. Sci. **65**: 339–350.

Kvile, K.i., D. Altin, L. Thommesen, and J. Titelman. 2021. Predation risk alters life history strategies in an oceanic copepod. Ecology **102**: e03214.

Langan, J. A., G. Puggioni, C. A. Oviatt, M. E. Henderson, and J. S. Collie. 2021. Climate alters the migration phenology of coastal marine species. Mar. Ecol. Prog. Ser. **660**: 1–18.

Maps, F., J. A. Runge, A. Leising, A. J. Pershing, N. R. Record, S. Plourde, and J. J. Pierson. 2012. Modelling the timing and duration of dormancy in populations of *Calanus finmarchicus* from the Northwest Atlantic shelf. J. Plankton Res. **34**: 36–54.

Meise, C., and J. O'Reilly. 1996. Spatial and seasonal patterns in abundance and age-composition of *Calanus finmarchicus*

in the Gulf of Maine and on Georges Bank: 1977–1987. Deep-Sea Res. II Top. Stud. Oceanogr. **43**: 1473–1501.

Melle, W., and others. 2014. The North Atlantic Ocean as habitat for *Calanus finmarchicus*: Environmental factors and life history traits. Prog. Oceanogr. **129**: 244–284.

Meyer-Gutbrod, E. L., and C. H. Greene. 2018. Uncertain recovery of the North Atlantic right whale in a changing ocean. Glob. Chang. Biol. **24**: 455–464.

Meyer-Gutbrod, E., C. Greene, K. Davies, and D. Johns. 2021. Ocean regime shift is driving collapse of the North Atlantic right whale population. Oceanography **34**: 22–31.

NASA Goddard Space Flight Center, Ocean Ecology Laboratory, Ocean Biology Processing Group 2020. MODIS-Terra Ocean Color Data; NASA Goddard Space Flight Center, Ocean Ecology Laboratory, Ocean Biology Processing Group. http://dx.doi.org/10.5067/TERRA/MODIS_OC.2014.0

US DOC/NOAA/NMFS. Zooplankton and ichthyoplankton abundance and distribution in the North Atlantic collected by the Ecosystem Monitoring (EcoMon) Project from 1977-02-13 to 2021-11-15(NCEI Accession 0187513). NOAA National Centers for Environmental Information. Dataset. https://www.ncei.noaa.gov/archive/accession/0187513.

Ohman, M. D., and H.-J. Hirche. 2001. Density-dependent mortality in an oceanic copepod population. Nature **412**: 638–641.

Pedersen, E. J., D. L. Miller, G. L. Simpson, and N. Ross. 2019. Hierarchical generalized additive models in ecology: An introduction with mgcv. PeerJ **7**: e6876.

Pershing, A. J., and others. 2021. Climate impacts on the Gulf of Maine ecosystem. Elementa: Sci. Anthropocene **9**: 00076.

Pershing, A. J., and A. Kemberling. 2023. Decadal comparisons identify the drivers of persistent changes in the zooplankton community structure in the northwest Atlantic. ICES J. Mar. Sci. **0**: 1–11.

Pierson, J. J., H. Batchelder, W. Saumweber, A. Leising, and J. Runge. 2013. The impact of increasing temperatures on dormancy duration in *Calanus finmarchicus*. J. Plankton Res. **35**: 504–512.

Plourde, S., and J. Runge. 1993. Reproduction of the planktonic copepod *Calanus finmarchicus* in the Lower St. Lawrence Estuary: Relation to the cycle of phytoplankton production and evidence for a *Calanus* pump. Mar. Ecol. Prog. Ser. **102**: 217–227.

Ratnarajah, L., and others. 2023. Monitoring and modelling marine zooplankton in a changing climate. Nat. Commun. **14**: 564.

Record, N., and others. 2019. Rapid climate-driven circulation changes threaten conservation of endangered North Atlantic right whales. Oceanography **32**: 162–169.

Record, N., A. Pershing, and D. Rasher. 2024. Early warning of a cold wave in the Gulf of Maine. Oceanography **37**: 1–4.

Ross, C. H., J. A. Runge, J. J. Roberts, D. C. Brady, B. Tupper, and N. R. Record. 2023. Estimating North Atlantic right whale prey based on *Calanus finmarchicus* thresholds. Mar. Ecol. Prog. Ser. **703**: 1–16.

Runge, J., S. Plourde, P. Joly, B. Niehoff, and E. Durbin. 2006. Characteristics of egg production of the planktonic copepod, *Calanus finmarchicus*, on Georges Bank: 1994–1999. Deep-Sea Res. II Top. Stud. Oceanogr. **53**: 2618–2631.

Runge, J. A., R. Ji, C. R. Thompson, N. R. Record, C. Chen, D. C. Vandemark, J. E. Salisbury, and F. Maps. 2015. Persistence of *Calanus finmarchicus* in the western Gulf of Maine during recent extreme warming. J. Plankton Res. **37**: 221–232.

Saumweber, W. J., and E. G. Durbin. 2006. Estimating potential diapause duration in *Calanus finmarchicus*. Deep-Sea Res. II Top. Stud. Oceanogr. **53**: 2597–2617.

Skjoldal, H. R., J. M. Aarflot, E. Bagøien, Y. Skagseth, J. Rønning, and V. S. Lien. 2021. Seasonal and interannual variability in abundance and population development of *Calanus finmarchicus* at the western entrance to the Barents Sea, 1995–2019. Prog. Oceanogr. **195**: 102574.

Skottene, E., A. M. Tarrant, D. Altin, R. E. Olsen, M. Choquet, and K. Kvile. 2020. Lipid metabolism in *Calanus finmarchicus* is sensitive to variations in predation risk and food availability. Sci. Rep. **10**: 22322.

Sorochan, K. A., S. Plourde, M. F. Baumgartner, and C. L. Johnson. 2021. Availability, supply, and aggregation of prey (*Calanus* spp.) in foraging areas of the North Atlantic right whale (*Eubalaena glacialis*). ICES J. Mar. Sci. **78**: 3498–3520.

Staudinger, M. D., and others. 2020. The role of sand lances (*Ammodytes* sp.) in the Northwest Atlantic ecosystem: A synthesis of current knowledge with implications for conservation and management. Fish Fish. **21**: 522–556.

Sydeman, W. J., and S. J. Bograd. 2009. Marine ecosystems, climate and phenology: Introduction. Mar. Ecol. Prog. Ser. **393**: 185–188.

Volterra, V. 1926. Fluctuations in the abundance of a species considered mathematically. Nature **118**: 558–560.

Wiebe, P. H., M. F. Baumgartner, N. J. Copley, G. L. Lawson, C. S. Davis, R. Ji, and C. H. Greene. 2022. Does predation control the diapausing stock of *Calanus finmarchicus* in the Gulf of Maine? Prog. Oceanogr. **206**: 102861.

Wood, S. N. 2017. *Generalized additive models: An introduction with R*. Chapman & Hall/CRC texts in statistical science, second ed. CRC Press/Taylor & Francis Group.

Acknowledgments

The authors acknowledge funding support from the Department of Defense through the National Defense Science & Engineering Graduate Fellowship Program, the Northeast U.S. Shelf Long Term Ecological Research (NES-LTER) Project (NSF OCE-1655686), U.S. National Oceanic and Atmospheric Administration Projects (NA21OAR4170379, NA22OAR4310557, and NA24OARX4320008), and BOEM Cooperative Agreements M19AC00022 and M23AC00010-00. The MARMAP/EcoMon dataset was provided by the U.S. National Marine Fisheries Services

through H. Walsh. The authors thank Natalie Renier (WHOI Creative Studio) for providing the scientific illustration used in Figure 5.

Conflict of Interest

None declared.

Submitted 02 July 2024
Revised 02 October 2024
Accepted 09 November 2024

Associate editor: Joseph Warren